Contribution from Chemistry Department A,
Technical University of Denmark, DK-2800 Lyngby, Denmark

Complex Formation in Pyrosulfate Melts. 1. Potentiometric, Cryoscopic, and Spectrophotometric Investigations of the Systems $K_2S_2O_7$-K_2SO_4 and $K_2S_2O_7$-K_2SO_4-V_2O_5 in the Temperature Range 410-450 °C

NIELS HOLGER HANSEN, RASMUS FEHRMANN, and NIELS J. BJERRUM*

Received February 9, 1981

By potentiometric measurements the mole fractions of K_2SO_4 in $K_2S_2O_7$-K_2SO_4 melts saturated with K_2SO_4 at 420, 430, 440, and 450 °C were found to be 0.038 58 (9) (i.e., 0.038 58 ± 0.000 09), 0.042 49 (10), 0.046 36 (7), and 0.050 52 (30), respectively. A plot of $-pK_s$ (where K_s is the solubility product of K^+ and SO_4^{2-}) vs. the inverse absolute temperature in the above temperature range was linear within the experimental error. From this plot $\Delta H°$ and $\Delta S°$ for the dissolution of K_2SO_4 in $K_2S_2O_7$ were calculated to be 35.21 (44) kJ/mol and 88.41 (63) J/(mol deg), respectively. The freezing-point constant, the enthalpy of fusion, and the melting point for $K_2S_2O_7$ were found by cryoscopic measurements of $K_2S_2O_7$ with additions of K_2SO_4 to be 50.791 (85) °C kg/mol, 19.931 (12) kJ/mol, and 418.8 (5) °C, respectively. The dissolution of vanadium(V) in $K_2S_2O_7$-K_2SO_4-V_2O_5 melts at 410-450 °C was investigated by potentiometric, cryoscopic, and spectrophotometric methods and could best be explained (under the assumption of formation of oxo sulfato complexes only) by the reactions $V_2O_5 + nS_2O_7^{2-} \rightarrow 2VO_{(5-n)/2}(SO_4)_n^{n-}$ and $VO_{(5-n)/2}(SO_4)_n^{n-} + SO_4^{2-} \rightleftarrows VO_2(SO_4)_2^{3-} + ((n-1)/2)S_2O_7^{2-}$, $n = 1$ or 3. At 430 °C, the pK value for $n = 1$ based on molar concentrations was found by spectrophotometry to be -0.62 (95% confidence limits -0.25 to -0.95), while the potentiometric measurements at 450 °C gave a pK value of -0.66 (95% confidence limits -0.60 to -0.71). The absorption spectra of the species system $VO(SO_4)_3^{3-}$-$VO_2SO_4^-$ (it was not possible to distinguish between these species) and $VO_2(SO_4)_2^{3-}$ are calculated from the observed spectra. A possible alternative formulation of the $VO(SO_4)_3^{3-}$ species is $VO_2SO_4S_2O_7^{3-}$.

Introduction

The oxidation of SO_2 to SO_3 catalyzed by vanadium oxides dissolved in potassium pyrosulfate melts is a key process to the chemical industry (sulfuric acid by the contact process). Nevertheless the reaction mechanism is still unresolved, and virtually nothing is known regarding the complex formation in the melt systems.[1,2] The liquid nature of the catalyst was first recognized in 1940,[3] and it is generally accepted that the catalytic activity of vanadium is due to the change in oxidation state between +5 and +4. The activity of the molten catalyst depends on the alkali metal cation present and increases with the ion radius of the alkali metal.[4,5] This seems to be connected with the increasing stability of higher pyrosulfates. It is furthermore clear that high catalytic activity is closely related to the ability of the catalyst to stabilize the vanadium in the +5 oxidation state (see ref 1 and references therein).

At present it seems likely that at least a three-step mechanism involving more than one V(IV) species must be considered[1,6,7] in order to describe the reaction. Furthermore, it seems necessary to include a step involving the precipitation of a catalytically inactive V(IV) species.[6,8]

The phase diagrams of the binary systems V_2O_5-$K_2S_2O_7$[9,10] and V_2O_5-K_2SO_4[10] have been examined. These systems, however, will only to a limited extent represent the industrial reaction compositions, as the system must be characterized by at least five components, for example, K_2SO_4, SO_3, V(IV), V(V), and H_2O (or $KHSO_4$). The lack of consistency in the phase investigations[11] and the difficulty in relating the results to the catalytic melts both seem to indicate that the identification of the catalytically active species must be based on investigations of the complex formation of vanadium in melt solutions and not in quenched crystalline phases.

The present paper constitutes the first part of a study of the solution chemistry of the catalytically important vanadium oxide-potassium pyrosulfate melts. The complex formation of vanadium(V) in dilute solutions of V_2O_5 in $K_2S_2O_7$-K_2SO_4 has been examined by three different techniques (i.e., potentiometry, cryoscopy, and spectrophotometry). The industrial process operates under nonequilibrium conditions further complicated because of gases (SO_2, O_2, SO_3) diffusing in and out of the melt dispersed in a porous solid. Also the present V(V) concentrations are considerably smaller than the ones used industrially. Hence, the present results although important do not reflect the exact industrial conditions.

The solution chemistry of vanadium(V) in aqueous media is very complicated, as indicated by numerous investigations.[12] Contrary to this, only few investigations apply to nonaqueous solutions; the most reliable of these concern the conditions in 100% H_2SO_4 and oleum.[13-15] In these solutions V(V) is present as VO^{3+} and VO_2^+ species coordinated to solvent ions forming tetrahedral, pentacoordinated, or octahedral complexes. The only investigation so far dealing with sulfate-containing melts[16] indicates that the species VO_2^+ and $VO_2SO_4^-$ are formed in molten NH_4HSO_4 at 200 °C. The well-known tendency of vanadium(V) to polymerize increases with the basicity of the solution. Probably no polymerization takes place in the acidity range that applies to the present melts.[13-15]

In connection with the present work it has been necessary also to investigate the solvent system $K_2S_2O_7$-K_2SO_4. The autodissociation of $K_2S_2O_7$ has been examined in several pa-

(1) Villadsen, J.; Livbjerg, H. *Catal. Rev.—Sci. Eng.* **1978**, *17*, 203.
(2) Kenney, C. N. *Catal. Rev.—Sci. Eng.* **1975**, *11*, 197.
(3) Frazer, J. H.; Kirkpatrick, W. J. *J. Am. Chem. Soc.* **1940**, *62*, 1659.
(4) Topsøe, H. F. A.; Nielsen, A. *Trans. Danish Acad. Tech. Sci.* **1948**, *1*, 3.
(5) (a) Tandy, G. H. *J. Appl. Chem.* **1956**, *6*, 68. (b) Jisu, P.; Tomkova, P.; Jara, V.; Vankova, V. *Z. Anorg. Allg. Chem.* **1960**, *303*, 121.
(6) Holroyd, F. P. B.; Kenney, C. N. *Chem. Eng. Sci.* **1971**, *26*, 1971.
(7) Boreskov, G. K.; Polyakova, G. M.; Ivanov, A. A.; Mastikhin, V. M. *Dokl. Akad. Nauk SSSR* **1973**, *210*, 626.
(8) Grydgaard, P.; Jensen-Holm, H.; Livbjerg, H.; Villadsen, J. *ACS Symp. Ser.* **1978**, *No. 65*, 582.
(9) Bazarova, Zh. G.; Boreskov, G. K.; Kefeli, L. M.; Karakchiev, L. G.; Ostankowich, A. A. *Dokl. Akad. Nauk SSSR* **1968**, *180*, 1132.
(10) Hähle, S.; Meisel, A. *Kinet. Katal.* **1971**, *12*, 1276.
(11) Hansen, N. H., Thesis, Chemistry Department A, The Technical University of Denmark, 1979.
(12) Pope, M. T.; Dale, B. W. *Q. Rev., Chem. Soc.* **1968**, *22*, 527.
(13) Mishra, H. C.; Symons, M. C. R. *J. Chem. Soc.* **1962**, 4411.
(14) Gillespie, R. J.; Kapoor, R.; Robinson, E. A. *Can. J. Chem.* **1966**, *44*, 1203.
(15) Paul, R. C.; Puri, J. E.; Malhotra, H. C. *J. Inorg. Nucl. Chem.* **1971**, *33*, 4191.
(16) Ben Hadid, A.; Picard, G.; Vedel, J. *J. Electroanal. Chem. Interfacial Electrochem.* **1976**, *74*, 157.

0020-1669/82/1321-0744$01.25/0

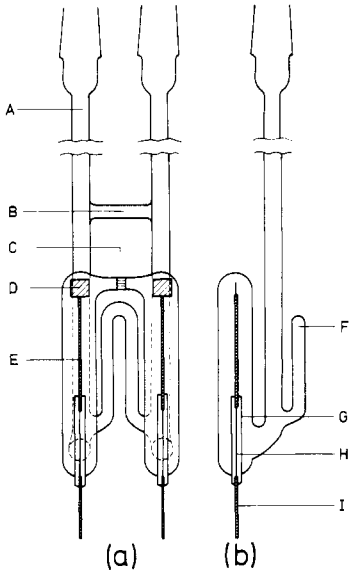

Figure 1. (a) Empty electrode cell of Pyrex, front view: A, neck; B, support rod; C, borosilicate filter; D, gold electrode plate; E, gold wire. (b) Empty electrode cell of Pyrex, side view: F, connection tube to equilibrate the pressure; G, Pyrex sealing; H, gold foil; I, gold wire.

pers.[17-21] The equilibrium constant $K_p = a_{SO_4^{2-}} P_{SO_3} / a_{S_2O_7^{2-}}$ (a and P have their usual meaning) has been calculated for $K_2S_2O_7$–K_2SO_4 melts at known partial pressures of SO_3 by either thermogravimetry[17,18] or electrochemical methods.[19-21] The K_p values thus obtained are rather inconsistent, and the experimental uncertainties are rather high. Finally, it seems that no special precautions have been taken to avoid contamination of the very hygroscopic $K_2S_2O_7$ with H_2O, thereby enhancing the solubility of K_2SO_4 in the melt.

Experimental Section

Materials. Pure $K_2S_2O_7$ was made by thermal dissociation of analytical grade $K_2S_2O_8$ from Merck (Pro Analysi, maximum 0.001% N) at 290 °C for $^1/_2$ h[22] in a stream of dry N_2 in order to avoid contamination by H_2O.[23] By weighing it was confirmed that $K_2S_2O_7$ did not give off any SO_3 at the temperature applied. K_2SO_4 (Merck, Suprapur) was dried at 300 °C. V_2O_5 (Merck, Extra Pure) was recrystallized in a quartz ampule and sealed off under 0.7 atm of oxygen (99.8% O_2, 0.2% N_2 + Ar), by heating to 700 °C followed by slow cooling (5 °C/h) to room temperature. Alternatively, sized granules from Cerac (Pure (99.9%)) were used without further treatment. All handling of chemicals took place in a nitrogen-filled glovebox with a measured water content of about 5 ppm (Panametric Standard Hygrometer) and continuous gas purification by forced recirculation through external molecular sieves. For the avoidance of hydrogen sulfate formation, $K_2S_2O_7$ was transferred immediately after synthesis to sealed ampules until used.

Potentiometry. The electrochemical cells were made of Pyrex with gold electrodes fused into the bottom. Contrary to platinum and the glassy carbon rods used for previous investigations in molten chloroaluminates,[23,24] gold was found to be inert to the pyrosulfate melts. This was tested by adding a weighed amount of the electrode material to an ampule containing a $K_2S_2O_7$–$KHSO_4$ (40:60 mol %) mixture. The ampule was sealed off under vacuum and heated to 430 °C for 24 h, and the possible weight loss of the electrode material was determined.

An empty Pyrex cell is shown in Figure 1. It consists of two compartments separated by a Sovirel borosilicate filter (C) of porosity 5. Before the cell was used, the filter resistance was tested by a 0.1 M K_2SO_4 solution. This is necessary because the filter sinters somewhat when fused into the cell, and hence the resistance may become too large. During operation the internal resistances of the cells were usually in the range 1000–5000 Ω.

The cell is equipped with two necks (A) made of 300-mm lengths of 8-mm tubing with standard taper joints on top. The gold electrodes are sealed vacuum-tight into the cell compartments by a very thin (15-μm) gold foil (H) fused into Pyrex (G), which is fused on the 1-mm diameter gold threads (E, I). The cells were filled with oxygen at 0.4 atm and sealed vacuum-tight. So that errors due to differences in vapor pressure above the melts might be eliminated, the tube (F) connecting the two cell compartments was sealed after oxygen had been added.

The potentiometric furnace and its regulation have been described in detail previously.[25] The cell was placed in the furnace in such a way that the melt was not in contact with the Pyrex sealing (G). Measurements of cell potentials took place with the furnace in a vertical position with the melts in the cell compartments in contact via the Pyrex filter, and equilibrium was reached after 3–30 days. The criterion for having attained equilibrium was that two measurements 24 h apart showed a difference of 0.01 mV or less.

The melt systems were investigated by the addition method, where the composition of one compartment (the measuring chamber) was changed by additions through the stems (A). This procedure implies that the stems of both compartments are cut and that both stems are sealed simultaneously under 0.4 atm of O_2. As the vapor pressures at room temperature are extremely low, no change in composition occurred by the evacuation. Six to eight additions could be made to each cell.

Cryoscopy. The cryoscopic measurements were performed by a special closed-cell technique based on momentarily local cooling. The cryoscopic cell was made of Pyrex. The cell compartment consisted of a 130-mm length of 30-mm (outer diameter) tubing, provided with a pocket of 8-mm tubing with a length of 40 mm. Into this pocket was fused a Pt resistance thermometer from Degussa. The empty cell was equipped with a 300-mm length of 8-mm tubing with a standard taper joint, permitting about eight successive additions of chemicals followed by sealing under vacuum.

The temperature could be determined with a relative accuracy of 0.03 °C (corresponding to 0.01 Ω), while the absolute accuracy was around 0.15–0.20 °C. However, it is the relative accuracy that is important in cryoscopic measurements. The Pt threads coming from the resistance thermometer were hard-soldered to two Au wires (diameter 1 mm), and each of these was again hard-soldered to Ag wires leading to a digital voltmeter that measured the resistance on the basis of a generated current of 1 mA. When additions were made to the cell, the Au wires were cut and resoldered. It was determined that the resistance did not change by this operation, as the melting points could be reproduced within 0.03 °C.

The measurements were performed by filling the cell (in a glovebox) with a sufficient amount of chemicals to result in a melt level 1–2 cm above the tip of the resistance thermometer. This corresponds to ca. 65 g of melt, giving a very large thermal mass to ensure the reproducibility. The cell was placed in a furnace similar to the ones used for the potentiometric measurements, and the melt was equilibrated 1–2 °C above the expected melting point.

It was not found suitable to solidify the melt just by lowering the furnace temperature, as a subcooling of ca. 30 °C was necessary. Alternatively, crystals were formed by spot cooling, a procedure by which the outer cell wall was contacted with a copper rod for ca. 30 s, having subcooled the melt 0.1–0.2 °C beforehand. By this technique, a transitory temperature drop of 0.5–2 °C was observed. The temperature then rose to the melting point and remained constant here within 0.03 °C for 15–30 min. The obtained melting point was only accepted if it could be reproduced within 0.03 °C, employing two different levels of subcooling. This could be achieved at subcoolings up to 2 °C, indicating that the heat loss through the soldered Au and Ag wires is negligible.

Spectrophotometry. The optical cells used for the spectrophotometric measurements were of fused quartz (Ultrasil from Helma or

(17) Coats, A. W.; Dear, D. J. A.; Penfold, D. *J. Inst. Fuel* **1968**, *41*, 129.
(18) Flood, H.; Førland, T. *Acta Chem. Scand.* **1947**, *1*, 781.
(19) Flood, H.; Boye, N. C. *Z. Elektrochem.* **1962**, *66*, 186.
(20) Comtat,, M.; Coubet, C.; Mahenc, J. *J. Electroanal. Chem. Interfacial Electrochem.* **1972**, *40*, 167.
(21) Durand, A.; Picard, G.; Vedel, J. *J. Electroanal. Chem. Interfacial Electrochem.* **1976**, *70*, 55.
(22) Baumgarten, P.; Thilo, E. *Ber. Dtsch. Chem. Ges. B* **1938**, *71*, 2596.
(23) von Barner, J. H.; Bjerrum, N. J. *Inorg. Chem.* **1973**, *12*, 1891.
(24) Brekke, P. B.; von Barner, J. H.; Bjerrum, N. J. *Inorg. Chem.* **1979**, *18*, 1372.
(25) Andreasen, H. A.; Bjerrum, N. J.; Foverskov, C. E. *Rev. Sci. Instrum.* **1977**, *48*, 1340.

Spectrosil from Thermal Syndicate) and had known path lengths of either ca. 1, ca. 0.5, or ca. 0.1 mm. The path lengths of about 0.1 mm were obtained by placing a precision-ground fused-silica insert into 5-mm cells. The cells were filled with chemicals in a glovebox and sealed under vacuum. Before the spectra were recorded, the cells were placed in spectrophotometric furnaces where the melts were equilibrated for 3–20 days at the measuring temperature. Equilibrium was reached when two measurements 24 h apart showed no change in absorbance (i.e., ≤0.003). The spectra were measured with a modified Cary 14R spectrophotometer equipped with furnaces rather similar to the furnaces described previously.[26] The furnaces were regulated to within ±0.1 °C with homemade PID regulators built to our requirements. The temperatures were measured by either calibrated chromel–alumel thermocouples or Pt resistance thermometers. The spectrophotometer was equipped with a Datex digital system for reading out the recorded spectra on paper tape.

Methods of Investigation

General Considerations. The formality C' is defined as the initial molar amount of one of the added substances (in the present work $K_2S_2O_7$, K_2SO_4, and V_2O_5) dissolved in 1 L of the melt. $C_{V(V)}$ is the molar concentration of vanadium in the oxidation state +5 (produced by addition of V_2O_5). The acid/base properties of the melts are characterized by the Lux–Flood concept[27,28] base ⇄ acid + O^{2-}. Hence, $S_2O_7^{2-}$ is a strong acid and SO_4^{2-} the corresponding base, according to eq 1. The densities of the melts used were calculated from

$$2SO_4^{2-} \rightleftarrows S_2O_7^{2-} + O^{2-} \quad (1)$$

the assumption that mixtures of $K_2S_2O_7$, K_2SO_4, and V_2O_5 behave ideally. As the amounts of V_2O_5 and K_2SO_4 were small compared to $K_2S_2O_7$, this assumption gives rise to only a small error. The densities of $K_2S_2O_7$, K_2SO_4, and V_2O_5 were obtained by the work of Hansen and Bjerrum,[29] Jaeger,[30] and Pantony and Vasu,[31] respectively.

Cell Potentials. The potentiometric investigations were performed by measuring the oxide activity in concentration cells with the compositions

Au I	1 atm O_2	solution I $K_2S_2O_7$–K_2SO_4 *or* $K_2S_2O_7$–K_2SO_4–V_2O_5	Pyrex filter	solution II K_2SO_4–$K_2S_2O_7$ saturated with K_2SO_4	1 atm O_2	Au II

So that a stable reference potential might be obtained, cell compartment II is always saturated with K_2SO_4. The electrode process at each electrode is considered to be $O_2 + 4e^- \rightleftarrows 2O^{2-}$, relating all data to the redox couple O_2/O^{2-}. The general equation for the cell potential is given by eq 2[32] since the

$$\Delta E = \frac{1}{F}\int_{I}^{II}\sum_i t_i\left(-z_i^{-1}d\mu_i - \frac{2}{4}d\mu_{O^{2-}}\right) \quad (2)$$

oxygen pressure, and hence the oxygen activity, is the same in both compartments. t_i, z_i, and μ_i are the transference number, charge, and chemical potential for the ith ion, respectively.

In molten $K_2S_2O_7$–K_2SO_4 the ions present are K^+, $S_2O_7^{2-}$, and SO_4^{2-}. The transference numbers are unknown but are considered constant for K^+ and $S_2O_7^{2-}$, as the concentration of these ions varies very little by the addition of K_2SO_4. The concentration of SO_4^{2-} and O^{2-} varies much but is small. It is a reasonable assumption to regard the transference numbers of these species as being proportional to the concentrations and hence the activities. After substitution and integration, eq 3 can then be written, where $t^\circ_{K^+}$ and $t^\circ_{S_2O_7^{2-}}$ are the

$$\Delta E = \frac{-RT}{2F}\ln\frac{[O^{2-}]_{II}}{[O^{2-}]_I} - \frac{RT}{F}t^\circ_{K^+}\ln\frac{[K^+]_{II}}{[K^+]_I} + \frac{RT}{2F}t^\circ_{S_2O_7^{2-}}\ln\frac{[S_2O_7^{2-}]_{II}}{[S_2O_7^{2-}]_I} + \frac{RT}{2F}k_{SO_4^{2-}}([SO_4^{2-}]_{II} - [SO_4^{2-}]_I) + \frac{RT}{2F}k_{O^{2-}}([O^{2-}]_{II} - [O^{2-}]_I) \quad (3)$$

transference numbers in pure $K_2S_2O_7$, and $k_{O^{2-}}$ and $k_{SO_4^{2-}}$ are constants, which by multiplication with the respective concentrations give the transference numbers for the species. The absolute values for the t° and k values are not known, but if the assumption is made, as was done previously, that the worst case[33,34] is for the mobility of the ions being independent of charge and inversely proportional to ion radius, the order of magnitude of the last four terms in eq 3 can be estimated. These terms will under all circumstances be small.

In the calculations the variations in activity coefficients have been neglected. This is reasonable since the ionic strength of the solvent is high ($K_2S_2O_7$ is completely dissociated, and the concentration is practically the same in both cell compartments).

On this basis, and with the ionic radii of K^+, $S_2O_7^{2-}$, SO_4^{2-}, and O^{2-} assumed to be 1.4, 6.0, 3.0, and 1.4 Å, respectively, the sum of the last four terms in eq 3 can be calculated as having a maximum value of –0.30 mV (the individual values are –0.80, –0.08, 0.58, and 0.00 mV, respectively). This calculation is based on a formal concentration of K^+, $S_2O_7^{2-}$, SO_4^{2-}, and O^{2-} in compartment I of 16.55, 8.26, 0.0142, and ~0 mol/L and in compartment II of 16.79, 8.04, 0.356, and ~0 mol/L, respectively. The sum of the last four terms in eq 3 is small compared with the maximum $|\Delta E|$ obtainable in these systems and is consequently neglected.

The expression for the cell potential, eq 3, then reduces to

$$\Delta E = \frac{-RT\ln 10}{2F}\log\frac{[O^{2-}]_{II}}{[O^{2-}]_I} \quad (4)$$

Sulfate and pyrosulfate are in equilibrium according to eq 1 and therefore

$$\Delta E = \frac{RT\ln 10}{F}\left(\log\frac{[SO_4^{2-}]_{II}}{[SO_4^{2-}]_I} + \log\left(\frac{[S_2O_7^{2-}]_I}{[S_2O_7^{2-}]_{II}}\right)^{1/2}\right) \quad (5)$$

and since $[S_2O_7^{2-}]$ to a good approximation is constant, the last term is close to zero and hence

$$pSO_4^{2-}(I) = -(F/(RT\ln 10))\Delta E + pSO_4^{2-}(II) \quad (6)$$

where $pSO_4^{2-}(I)$ and $pSO_4^{2-}(II)$ are the negative logarithms of the sulfate concentrations in cell compartments I and II, respectively. In the present case the maximum error by using eq 6 instead of eq 5 is 0.82 mV. This error is small enough to be neglected especially since part of this error is cancelled by neglecting the last four terms in eq 3. Equation 6 can also be applied to measurements on V_2O_5-containing $K_2S_2O_7$–K_2SO_4 melts, as the presuppositions made concerning the $K_2S_2O_7$–K_2SO_4 melts are still valid when adding small amounts of V_2O_5. From the measured pSO_4^{2-} of the melt, and from the formality of V(V), $\bar{n}$, the average experimental co-

(26) Fehrmann, R.; Bjerrum, N. J.; Andreasen, H. A. *Inorg. Chem.* **1975**, *14*, 2259.
(27) Lux, H. *Z. Elektrochem.* **1939**, *45*, 303.
(28) Flood, H.; Førland, T. *Acta Chem. Scand.* **1947**, *1*, 592.
(29) Hansen, N. H.; Bjerrum, N. J. *J. Chem. Eng. Data* **1981**, *26*, 195.
(30) Jaeger, F. M. *Z. Anorg. Allg. Chem.* **1917**, *101*, 1.
(31) Pantony, D. A.; Vasu, K. I. *J. Inorg. Nucl. Chem.* **1968**, *30*, 433.
(32) Guggenheim, E. A. "Thermodynamics"; North-Holland Publishing Co.: Amsterdam, 1967; pp 321–324.
(33) von Barner, J. H.; Bjerrum, N. J.; Kiens, K. *Inorg. Chem.* **1975**, *14*, 1807.
(34) Fehrmann, R.; Bjerrum, N. J.; Andreasen, H. A. *Inorg. Chem.* **1976**, *15*, 2187.

ordination number defined as

$$\bar{n} = (C'_{K_2SO_4} - [SO_4^{2-}])/C_{V(V)} \quad (7)$$

can be calculated.

Absorption Spectra. The molar absorptivity is defined by $A(lC)^{-1}$ where A is the absorbance corrected for the absorbance of cell and solvent, l is the path length, and C is the molar concentration. It can be shown from the Bouguer–Beer law and the law of additive absorbances that a general three-matrix equation can be put forward:[33,35]

$$(A_m(\nu'_n)) = (l_m C_{mi})(\epsilon_i(\nu'_n)) \quad (8)$$

where $A_m(\nu'_n)$ is the absorbance of the mth composition at the wavenumber ν'_n, l_m is the optical path length at the mth composition, C_{mi} is the concentration of the ith species at the mth composition, and $\epsilon_i(\nu'_n)$ is the molar absorptivity of the ith species at wavenumber ν'_n. If the number of different compositions o is larger than the number of species s, eq 8 results in an overdetermined equation system, from which $\epsilon_i(\nu'_n)$ can be calculated. The absorption spectra are, however, encumbered with absorption-dependent uncertainties, $\Delta A_m(\nu'_n)$, which in the first place imply that eq 8 does not have an exact solution for $o > s$. Another solution is to minimize the residual vector

$$V_m(\nu'_n) = A_m(\nu'_n) - l_m \sum_{i=1}^{s} C_{mi}\epsilon_i(\nu'_n) \qquad m = 1, 2, \ldots, o \quad (9)$$

$V_m(\nu'_n)$ should however first be weighed with the factor $(\Delta A_m(\nu'_n))^{-1}$. The minimal residual vector is thus obtained by determining the values of $\epsilon_i(\nu'_n)$ resulting in a minimal geometrical length of the residual vector, i.e., so that

$$S(\epsilon_i(\nu'_n)) = \sum_{m=1}^{o} ((\Delta A_m(\nu'_n))^{-1} V_m(\nu'_n))^2 \qquad \epsilon_i \geq 0 \quad (10)$$

obtains its smallest value.

From a given model and a given set of equilibrium constants, the best values of $\epsilon_i(\nu'_n)$ can thus be calculated. By systematic variation of the equilibrium constants, the combination of species concentrations C_{mi} and molar absorptivities $\epsilon_i(\nu'_n)$ resulting in minimal $S(\epsilon_i(\nu'_n))$ can be calculated. If the proposed model is correct, $S(\epsilon_i(\nu'_n))$ is now exclusively a result of uncertainties due to the apparatus (and other experimental uncertainties).

The above procedure has recently[36] been used in a new computer program, which is able to investigate generally up to 8 species (i.e., 6 equilibria) and 30 different spectra, each including 400 measured wavenumbers.

Cryoscopy. The freezing point depression, θ, for a solvent, to which are added minor amounts of foreign matter is determined by

$$\theta = \lambda m \quad (11)$$

where λ is the freezing point constant for the solvent and m is here the molality of added substances. The freezing point constant is given by

$$\lambda = \frac{MRT_0^2}{1000(\Delta H_{fus})} \quad (12)$$

where M is the molar mass of the solvent, R is the gas constant, T_0 is the freezing point of the solvent, and ΔH_{fus} is the enthalpy of fusion for the solvent. Equation 11 is generally valid only for small values of m, but nevertheless, in molten electrolytes proportionality between θ and m has been observed up to a content of 10 mol % of added substances.[37]

From the measured freezing point depressions of the melt, and from the molality of V(V), ν, the number of moles of particles produced in the melt per added mole of V(V) can be calculated with the employment of a value of λ calculated from freezing point measurements of $K_2S_2O_7$ with added K_2SO_4.

Table I. Values of Mole Fractions[a] and Cell Potentials for Molten $K_2S_2O_7$–K_2SO_4 in the Temperature Range 420–450 °C

mole fraction of K_2SO_4	$-\Delta E$, mV			
	420 °C	430 °C	440 °C	450 °C
0.001 45		195.07		
0.001 45		191.06		
0.002 80		168.55		
0.005 34		127.04		
0.006 93		110.71		
0.008 54		98.05		
0.012 41		74.82		
0.017 60	47.46	53.85	59.98	65.82
0.018 92		48.63		
0.026 48	22.87	29.05	34.81	40.74
0.033 76		14.0		
0.035 91	4.04	10.17	16.10	22.27
0.037 73		7.75		
0.040 14		3.61		

[a] Corrected for the presence of K_2SO_4 initially in the $K_2S_2O_7$ used.

Results and Discussion

Potentiometric Measurements of the System K_2SO_4–$K_2S_2O_7$ in the Temperature Range 420–450 °C. From the discussion under Methods of Investigation, it is obvious that in order to determine the pSO_4^{2-} in a given melt, it is necessary to know the sulfate concentration in the saturated melt used in the reference compartment. Near the saturation point, the amount of sulfate formed by the dissociation of pyrosulfate is small compared with the amount of K_2SO_4 added to cell compartment I and one should in accordance with eq 6 obtain a straight line with the slope of unity if $-(F/(RT \ln 10))\Delta E$ is plotted against the negative logarithm of the formality of the potassium sulfate added. The intercept at the abscissa (where $-\Delta E = 0$) will then give pSO_4^{2-}(II) at the chosen temperature. There are, however, two corrections that should be taken into consideration. It is highly probable that the $K_2S_2O_7$ employed is contaminated with small amounts of sulfate, inevitably formed during the electrolytic preparation of $K_2S_2O_8$, and this must be taken into account when determining pSO_4^{2-}(II). Further, far from the saturation point the sulfate formed by dissociation of $S_2O_7^{2-}$ to SO_4^{2-} and SO_3 (or $S_3O_{10}^{2-}$) makes a considerable contribution to the total sulfate content of the melt. By an iterative procedure using the criterion that straight lines should be obtained (for basic melts) both the initial $[SO_4^{2-}]$ and the pK value for the dissociation ($S_2O_7^{2-} \rightleftarrows SO_4^{2-} + SO_3$) were determined. Values of 0.0120 mol/L and 5.49 (20) were found, respectively, at 430 °C. It can be seen that the sulfate impurity is low (corresponding to a purity of the used pyrosulfate of 99.9%). It has, however, a considerable influence on the value of the dissociation constant.

In Table I are shown the values for the measured potentials, and Table II gives the values of $-(F/(RT \ln 10))\Delta E$ as a function of the negative logarithm of the formality of K_2SO_4 (corrected for initial $[SO_4^{2-}]$) at different temperatures. A plot of the values of Table II is given in Figure 2. The straight lines in this figure are drawn by use of a least-squares method, and the weighted average of the slopes for all the lines is found to be 1.007 (4). This indicates that the assumptions made to reach eq 6 are correct within the experimental uncertainties.

(35) Lieto, L. R., Thesis, 1969. Report ORNL-TM-2714: Oak Ridge National Laboratory: Oak Ridge, Tenn., 1969.
(36) Fehrmann, R.; Bjerrum, N. J.; Pedersen, E. *Inorg. Chem.*, in press.
(37) Kordes, E.; Bergmann, W.; Vogel, W. *Z. Elektrochem.* **1951**, *55*, 600.

Table II. Values Used To Obtain the Solubility of K_2SO_4 in $K_2S_2O_7$–K_2SO_4 Melts in the Temperature Range 420–450 °C

420 °C		430 °C				440 °C		450 °C	
$-\log C'_{K_2SO_4}$	$-F(\Delta E)/(RT \ln 10)$	$-\log C'_{K_2SO_4}$	$-F(\Delta E)/(RT \ln 10)$	$-\log C'_{K_2SO_4}$	$-F(\Delta E)/(RT \ln 10)$	$-\log C'_{K_2SO_4}$	$-F(\Delta E)/(RT \ln 10)$	$-\log C'_{K_2SO_4}$	$-F(\Delta E)/(RT \ln 10)$
0.8327	0.3451	1.3534	0.9104[a]	0.8024	0.3485	0.8354	0.4239	0.8368	0.4587
0.6539	0.1663	1.2401	0.7934[a]	0.6552	0.2082	0.6566	0.2460	0.6580	0.2839
0.5202	0.0294	1.1493	0.7027[a]	0.5487	0.1003	0.5229	0.1138	0.5243	0.1552
		0.9867	0.5362	0.4998	0.0555				
		0.8341	0.3860	0.4725	0.0259				

[a] Not included in Figure 3.

Table III. Composition of Saturated Melts in the Temperature Range 420–450 °C

temp, °C	pSO_4^{2-}	mole fraction $X_{K_2SO_4}$	variance × 10^8	$[K^+]$, mol/L	$[SO_4^{2-}]$, mol/L
420	0.4887 (11)	0.038 58 (9)	2.17	16.827	0.3246
430	0.4475 (10)	0.042 49 (10)	8.43	16.798	0.3569
440	0.4104 (7)	0.046 36 (7)	0.32	16.769	0.3887
450	0.3738 (26)	0.050 52 (30)	37.1	16.741	0.4229

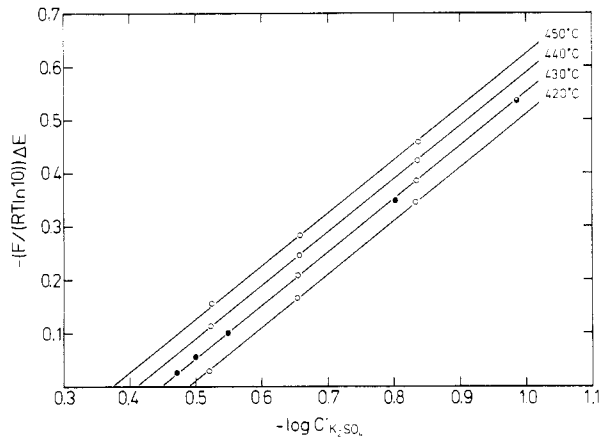

Figure 2. Plots used to check eq 6 for the K_2SO_4–$K_2S_2O_7$ system at 420, 430, 440, and 450 °C. Open circles, filled circles, and half-filled circles refer to the three electrode cells used.

The pSO_4^{2-} and the composition of the saturated melt at the measured temperatures can consequently[24] be calculated on the basis of straight lines with fixed slopes of unity. The results are shown in Table III, where also the molar concentrations of potassium ions and sulfate ions are given together with the variances. These variances—the experimental variances—are calculated from the deviations between the measured data points and the calculated straight lines and expressed in mole fraction units.

Since the melts are saturated, the product of the square of the concentration of potassium ions and sulfate ions should be constant at constant temperature, i.e.

$$[K^+]^2[SO_4^{2-}] = K_s \qquad (13)$$

K_s (the solubility product) can now be calculated from Table III and pK_s plotted vs. the inverse absolute temperature. Such a plot is shown in Figure 3. The data points follow a straight line within the experimental error, implying that the deviation from linearity expected from Kirchoff's law is small. On the basis of a regression analysis, the equation for the line was found to be $-pK_s = (-1839\ (23))T + 4.618\ (33)$.

It can be seen from Table III that the solubility of K_2SO_4 in $K_2S_2O_7$ is rather low. Very few data are available in the literature, but Durand et al.[21] have found a considerably higher solubility at 430 °C, i.e., a value of 0.062 for the mole fraction of K_2SO_4, employing a commercially available $K_2S_2O_7$. This deviation might be due to a content of $KHSO_4$ in the melt

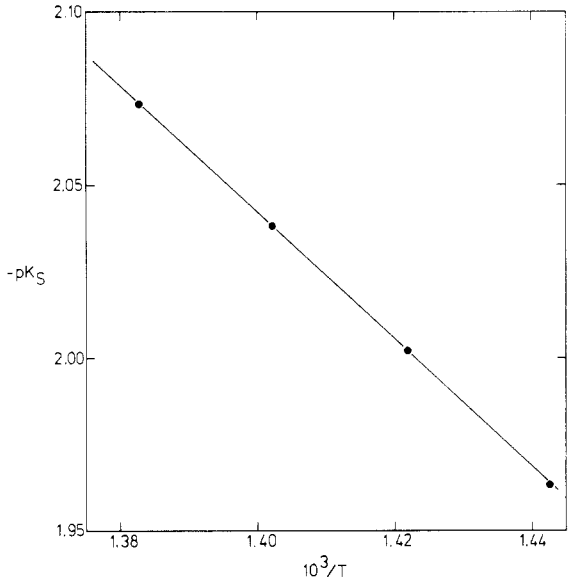

Figure 3. $-pK_s$ (K_s is the solubility product of K^+ and SO_4^{2-}) as a function of the inverse absolute temperature ($\times 10^3$). The straight line is drawn from a least-squares calculation using weighted values.

investigated by Durand et al., since commercial analytical grade $K_2S_2O_7$ investigated by Hansen[11] was shown to contain considerable amounts of $KHSO_4$. Addition of $KHSO_4$ to $K_2S_2O_7$ is known[38] to increase the solubility of K_2SO_4 markedly.

From the plot in Figure 3 it is possible to calculate $\Delta H°$ and $\Delta S°$ for the dissolution process $K_2SO_4(s) \rightleftarrows 2K^+(soln) + SO_4^{2-}(soln)$ within limited temperature ranges. The values are found to be 35.21 (44) kJ/mol and 88.41 (63) J/(mol deg), respectively. Since no direct calorimetric investigations seem to have been performed on this system, the best quantity with which to compare the obtained $\Delta H°$ value is the enthalpy of fusion of K_2SO_4 (where the solvent is K_2SO_4). This has been found to 36.8 kJ/mol,[39] and the similarity of this value and $\Delta H°$ indicates that the solution of K_2SO_4 in $K_2S_2O_7$ can be considered almost ideal.

A tentative value for the equilibrium constant, K_1, for the equilibrium

$$2S_2O_7^{2-} \rightleftarrows S_3O_{10}^{2-} + SO_4^{2-} \qquad (14)$$

can be obtained from the potentiometric measurements at 430 °C. However, only two of the data points can be considered to affect the calculation of K_1, and the calculated value of $pK_1 = 6.4$ must be taken as a provisional estimate. For comparison, we have calculated pK_1 to be 5.5 on the basis of the Durand et al.[21] data. The reason for suggesting that $K_2S_2O_7$ dissociates according to eq 14 rather than the equation $S_2O_7^{2-} \rightleftarrows SO_4^{2-} + SO_3$ is the observed high solubility of SO_3 in the melts.

(38) Hansen, N. H.; Fehrmann, R.; Bjerrum, N. J., to be submitted for publication.
(39) Rossini, S.; Wagmann, D. D.; Evans, W. H.; Levine, S.; Jaffe, I. *Natl. Bur. Stand. (U.S.), Circ.* **1952**, *No. 500.*

Table IV. Freezing Points of Solutions of K_2SO_4 and V_2O_5 in $K_2S_2O_7$ with Calculated ν Values

molality of K_2SO_4	molality of V_2O_5	temp, °C	θ, °C	θ_{rel}, °C	ν
0	0	418.52			
0.015 0_3	0	417.76	0.76		1
0.029 9_6	0	417.00	1.52		1
0.039 1_0	0	416.54	1.98		1
0.039 1_0	0.014 7_6	415.13	3.39	1.41	1.88
0.039 1_0	0.029 2_1	413.59	4.93	2.95	1.99
0.039 1_0	0.037 7_7	412.74	5.78	3.80	1.98
0	0	418.64			
0.102 7_7	0	413.59	5.05		1
0.102 7_7	0.015 0_8	412.74	5.90	0.85	1.10
0.102 7_7	0.028 6_0	411.72	6.92	1.87	1.28
0.102 7_7	0.037 3_3	411.05	7.59	2.54	1.34
0.102 7_7	0.073 4_7	407.87	10.77	5.72	1.53

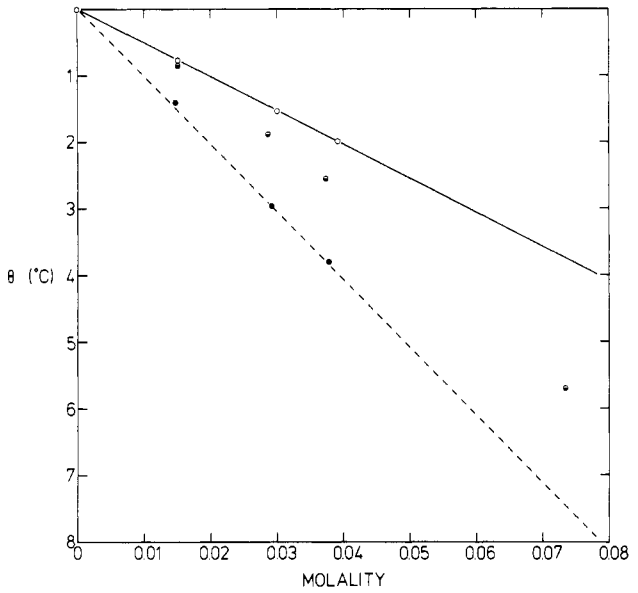

Figure 4. The freezing point depression of $K_2S_2O_7$ as a function of the molality of K_2SO_4 (open circles), the molality of V_2O_5 at $C'_{K_2SO_4}$ = 0.21 mol/L (half-filled circles), and the molality of V_2O_5 at $C'_{K_2SO_4}$ = 0.08 mol/L (filled circles). The dashed line is drawn with a slope corresponding to two particles produced per particle added. The straight line through the K_2SO_4 data points, representing a slope of one particle produced per particle added, is drawn from a least-squares analysis.

Furthermore, it has been shown by successively sealing off reservoirs with known volumes connected to the measuring chamber that the measured potentials are independent of the gas volumes above the melt, supporting the view that gaseous SO_3 does not significantly take part in the dissociation reactions. Finally, it is well-known that $K_2S_2O_7$ forms $K_2S_3O_{10}$ by uptake of SO_3.[22] It is, however, not possible on the basis of the computer calculations alone to decide whether SO_3 or $S_3O_{10}^{2-}$ is involved in the dissociation of $K_2S_2O_7$.

Cryoscopic Measurements of the Systems $K_2S_2O_7$–K_2SO_4 and $K_2S_2O_7$–K_2SO_4–V_2O_5. In Table IV are shown the measured freezing point depressions of $K_2S_2O_7$ with added K_2SO_4 and K_2SO_4–V_2O_5, and the results are shown in Figure 4. The freezing point constant for $K_2S_2O_7$ has been determined by addition of K_2SO_4, giving 1 mol of foreign particles/mol of K_2SO_4 added. It is seen from Figure 4 that the measured freezing point depressions follow a straight line, and from the slope the freezing point constant is calculated to be λ = 50.791 (85) °C kg/mol. By the substitution of 418.5 (5) °C for T_0 in eq 12, the enthalpy of fusion of $K_2S_2O_7$ is calculated to be

$$\Delta H_{fus} = 19.931\ (12)\ \text{kJ/mol}$$

No value for ΔH_{fus} can be found in the literature, but by a differential enthalpic analysis with a high-temperature Calvet calorimeter a value of 20.38 (67) kJ/mol has been determined,[40] agreeing very well with the above value.

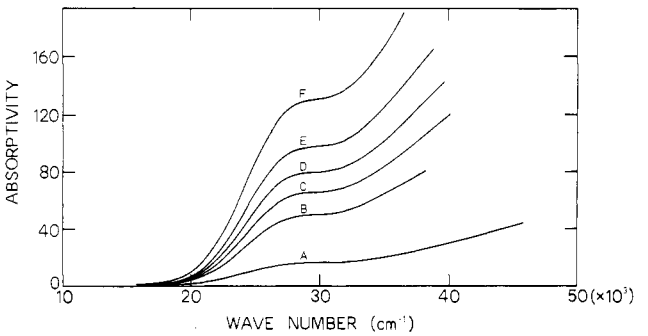

Figure 5. Series of spectra of V_2O_5 in $K_2S_2O_7$ at 430 °C. The concentration (in mol/L) of V(V) is as follows: A, 0.00478; B, 0.01477; C, 0.01979; D, 0.02494; E, 0.02993; F, 0.04071.

The dashed line in Figure 4 represents a freezing point depression of twice that found for K_2SO_4, and it is seen that this line is closely followed by V_2O_5 when added to very dilute solutions of K_2SO_4 in $K_2S_2O_7$. Thus, two new particles are produced in the melt for each V_2O_5 added. At higher concentrations of K_2SO_4, a smaller value of ν is obtained, illustrated in Figure 4 by the experimental points located between the lines. This indicates that some complex formation takes place between the vanadium species and sulfate ions, and that this complex formation is dependent on the sulfate activity of the melt. On the other hand, the cryoscopic results do not reveal anything about the nature of the particles formed, and so that more information might be obtained, spectrophotometric as well as potentiometric measurements were included in the investigations.

Spectrophotometric Measurements of V_2O_5 in $K_2S_2O_7$–K_2SO_4 Melts at 410–450 °C. The spectrophotometric measurements have been performed on several series of melts in order to investigate the influence on the complex formation of the formality of V_2O_5, the sulfate content, and the influence of the temperature.

The effect of the vanadium(V) concentration has been investigated by recording visible and ultraviolet spectra of V_2O_5 dissolved in $K_2S_2O_7$ in the concentration range $C_{V(V)}$ = 0.005–0.04 mol/L at 430 °C. The resultant spectra, corrected for absorption of $K_2S_2O_7$, background, and differences in optical path lengths, are shown in Figure 5. All the spectra exhibit the same features; i.e., one absorption band at approximately 29 × 10^3 cm^{-1} emerges as a shoulder of one or several very intense bands that could be charge-transfer bands with maxima in the far-ultraviolet. The Bouguer–Beer law is obeyed at all wavenumbers in the measured concentration range. It is consequently assumed that the nature of the vanadium(V) species present does not depend on the concentration in the measured molarity range, and this strongly suggests that only monomeric vanadium(V) species are formed by the dissolution of V_2O_5 in molten $K_2S_2O_7$.

The cryoscopic measurements indicate that the presence of sulfate in the melts has an effect on the vanadium(V) species formed. This phenomenon was further investigated spectrophotometrically, and in Figure 6 are shown the corrected spectra at 430 °C of V_2O_5 ($C_{V(V)}$ = 0.015 mol/L) dissolved in $K_2S_2O_7$ melts with a formality of K_2SO_4 of $C'_{K_2SO_4}$ = 0–0.3 mol/L. The spectra are here expressed by the molar absorptivity and show the same absorption bands as the spectra in Figure 5. However, a pronounced effect due to the differences in sulfate content can be observed. Apparently the

(40) Gaune-Escard, M., Laboratoire de Dynamique et Thermophysique des Fluides, Université de Provence, private communication.

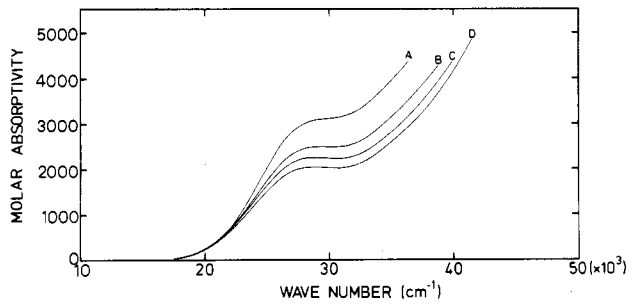

Figure 6. Series of spectra of 0.015 mol/L V(V) added as V_2O_5 in $K_2S_2O_7$–K_2SO_4 at 430 °C. The formal concentration (in mol/L) of K_2SO_4 is as follows: A, 0.012 07; B, 0.1191; C, 0.2132; D, 0.3117. The molar absorptivities are calculated on the basis of monomeric V(V).

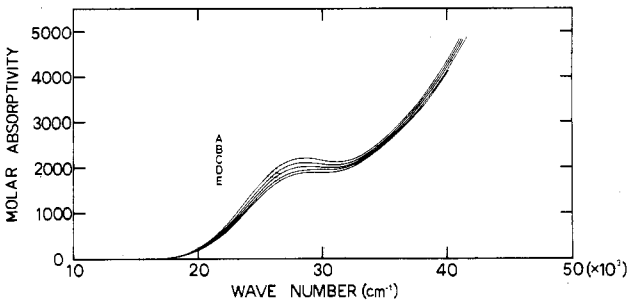

Figure 7. Series of spectra of 0.015 mol/L V(V) as V_2O_5 in $K_2S_2O_7$–K_2SO_4. Temperatures (in °C) and formal concentrations (in mol/L) of K_2SO_4 are as follows respectively: A, 410, 0.3137; B, 420, 0.3127; C, 430, 0.3117; D, 440, 0.3107; E, 450, 0.3097. The molar absorptivities are calculated on the basis of monomeric V(V).

intensity of the charge-transfer bands decreases by increasing the sulfate content, whereas the absorption band at ca. 29 × 10^3 cm^{-1} remains approximately constant (i.e., with absorbance due to charge-transfer bands subtracted).

The temperature effect is illustrated in Figure 7, showing spectra of $K_2S_2O_7$ melts at 410–450 °C with $C_{V(V)}$ = 0.015 mol/L and $C'_{K_2SO_4}$ = 0.31 mol/L. Here it seems that the absorption band at 29 × 10^3 cm^{-1} is rather temperature sensitive; it decreases markedly with increasing temperature. The charge-transfer bands are much less dependent on the temperature; only a slight decrease is observed with increasing temperature.

The above observations seem to indicate that at least three vanadium(V) species are involved. As mentioned under Methods of Investigation, the $K_2S_2O_7$ melt constitutes a strongly acidic medium in the Lux–Flood sense. According to the discussion in the Introduction, one would expect to encounter vanadium(V) species containing the entities VO_2^+ and VO^{3+} in very acidic media, with VO^{3+} as the strongest acid:

$$VO^{3+} + O^{2-} \rightleftarrows VO_2^+ \quad (15)$$

By addition of SO_4^{2-} to the $K_2S_2O_7$ melt, this will be more basic according to $S_2O_7^{2-} + O^{2-} \rightleftarrows 2SO_4^{2-}$, hence shifting eq 15 to the right. Under the assumption that the melts, even with maximum sulfate content, always remain sufficiently acidic to exclude the formation of other vanadium(V) entities, a reasonable explanation can be put forward to account for the spectrophotometric observations. The basis for this assumption will be further discussed in connection with the potentiometric investigations. It is not possible on the basis of the spectrophotometric data alone to determine the identities of the complexes formed.

When the tendency of VO^{3+} and VO_2^+ to form mainly octahedral (or tetrahedral) complexes is taken into account

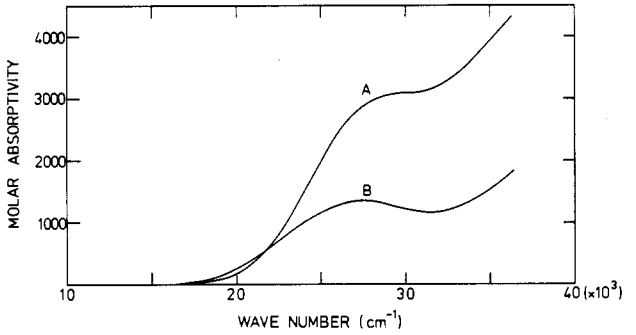

Figure 8. Calculated spectra of (A) the $VO_2SO_4^-$–$VO(SO_4)_3^{3-}$ (or $VO_2SO_4S_2O_7^{3-}$) system and (B) $VO_2(SO_4)_2^{3-}$. The solvent was $K_2S_2O_7$–K_2SO_4 at 430 °C. Each spectrum was calculated on the basis of six measured spectra by use of the pK values of −0.62 and −1.54 for the reactions $VO_2SO_4^- + SO_4^{2-} \rightleftarrows VO_2(SO_4)_2^{3-}$ and $VO(SO_4)_3^{3-} + SO_4^{2-} \rightleftarrows VO_2(SO_4)_2^{3-} + S_2O_7^{2-}$, respectively.

Table V. pK Values for the Equilibria $VO_2SO_4^- + SO_4^{2-} \rightleftarrows VO_2(SO_4)_2^{3-}$ (i) and $VO(SO_4)_3^{3-} + SO_4^{2-} \rightleftarrows VO_2(SO_4)_2^{3-} + S_2O_7^{2-}$ (ii) in Molten $K_2S_2O_7$–K_2SO_4

temp, °C	eq	pK	95% conf lim	variance × 10^5
430	i	−0.62[a]	−0.25 to −0.95	6.65
430	ii	−1.54[a]	−1.17 to −1.87	6.90
450	i	−0.66[b]	−0.60 to −0.71	197

[a] Based on spectrophotometric measurements for 0.05–0.15 mol/L V(V). The variance was calculated as absorptivity. [b] Based on potentiometric measurements at 0.15 mol/L V(V). The variance was calculated as $\bar{n}$.

and formation of oxo sulfato complexes only is assumed, eq 15 can be written as eq 16. The species $VO(SO_4)_3^{3-}$ can be

$$VO(SO_4)_3^{3-} + SO_4^{2-} \rightleftarrows VO_2(SO_4)_2^{3-} + S_2O_7^{2-} \quad (16)$$

regarded as a solvated complex according to eq 17. In this

$$VO_2SO_4^- + S_2O_7^{2-} \rightleftarrows VO(SO_4)_3^{3-} \quad (17)$$

connection it should be noted that if pyrosulfate ligands are also considered, an isomeric formulation for $VO(SO_4)_3^{3-}$ is $VO_2SO_4S_2O_7^{3-}$. With $K_2S_2O_7$ as solvent the dominating species accordingly will be either $VO(SO_4)_3^{3-}$ (or $VO_2SO_4S_2O_7^{3-}$) or $VO_2SO_4^-$. From the cryoscopic measurements, a cryoscopic factor of ν = 2 was observed in $K_2S_2O_7$ melts containing very little SO_4^{2-}, and this agrees with one of the following dissolution processes taking place:

$$V_2O_5 + S_2O_7^{2-} \rightarrow 2VO_2SO_4^- \quad (18)$$

$$V_2O_5 + 3S_2O_7^{2-} \rightarrow 2VO(SO_4)_3^{3-} \quad (19)$$

The features of Figures 6 and 7 can now be explained in the following way. The decrease in intensity of the charge-transfer bands with increasing sulfate concentration shown in Figure 6 is due to a decrease of the concentration of $VO(SO_4)_3^{3-}$ (and $VO_2SO_4^-$) and an increase of the concentration of $VO_2(SO_4)_2^{3-}$. The invariance in the 29 × 10^3 cm^{-1} band indicates that both $VO(SO_4)_3^{3-}$ and $VO_2(SO_4)_2^{3-}$ have a band close to this wavenumber. The decrease with increasing temperature of the 29 × 10^3 cm^{-1} band (while the charge-transfer bands remain almost constant) indicates a shift in eq 17 decreasing the concentration of $VO(SO_4)_3^{3-}$ with increasing temperature. Such a shift is also what would be expected.

A model for the complex formation of vanadium(V) in $K_2S_2O_7$–K_2SO_4 melts at 410–450 °C could then involve eq 16 and 20, with the formation of $VO_2SO_4^-$ preferred to $VO(SO_4)_3^{3-}$ (or $VO_2SO_4S_2O_7^{3-}$) at high temperatures.

$$VO_2SO_4^- + SO_4^{2-} \rightleftarrows VO_2(SO_4)_2^{3-} \quad (20)$$

Table VI. Values of Cell Potential and Composition of V_2O_5 in Molten $K_2S_2O_7$-K_2SO_4[a] at 410–450 °C

mole fraction (0.15 mol/L V(V))		$-\Delta E$, mV					
$K_2S_2O_7$	K_2SO_4	410 °C	415 °C	420 °C	430 °C	440 °C	450 °C
0.930 54	0.060 50						1.64
0.935 51	0.055 48						7.73
0.942 44	0.048 60				4.91	10.02	15.36
0.945 37	0.045 78						20.47
0.950 25	0.040 72	6.13	9.14	12.07	17.95	23.66	29.61
0.962 39	0.028 35						59.88
0.964 62	0.026 21	38.86	41.94	45.14	51.65	57.49	64.05
0.973 56	0.017 36						91.21
0.975 59	0.015 14						105.45
0.980 10	0.010 59						124.01
0.984 27	0.006 55						153.16
0.984 79	0.005 85						158.27

mole fraction (0.5 mol/L V(V))		$-\Delta E$, mV			mole fraction (0.7 mol/L V(V))		$-\Delta E$, mV	
$K_2S_2O_7$	K_2SO_4	415 °C	430 °C	450 °C	$K_2S_2O_7$	K_2SO_4	430 °C	450 °C
0.911 76	0.059 28			35.76	0.914 89	0.044 30	65.20	77.22
0.927 65	0.043 04	41.49	49.77	61.80				

[a] Corrected for K_2SO_4 initially present in the $K_2S_2O_7$ used.

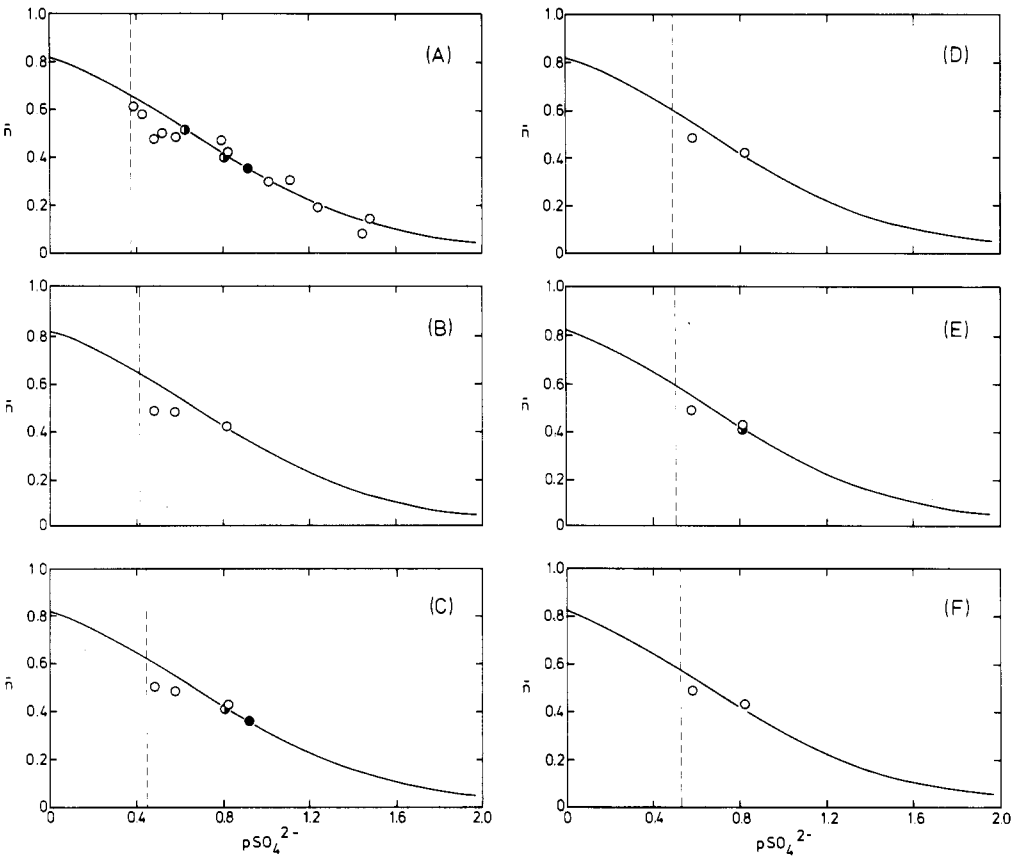

Figure 9. Average experimental coordination number ($\bar{n}$) for V(V) as a function of pSO_4^{2-}: A, 450 °C; B, 440 °C; C, 430 °C; D, 420 °C; E, 415 °C; F, 410 °C. Calculated curves are for the reaction $VO_2SO_4^- + SO_4^{2-} \rightleftarrows VO_2(SO_4)_2^{3-}$ at 450 °C and 0.15 mol/L V(V). The vertical dashed lines show the limiting pSO_4^{2-} due to saturation with K_2SO_4. Open circles represent 0.15 mol/L V(V), half-filled circles represent 0.5 (or 0.49–0.50) mol/L V(V), and filled circles represent 0.7 (or 0.69–0.70) mol/L V(V).

As discussed under Methods of Investigation it is possible to calculate the spectrum of each species for any particular model at a given temperature. This has been done at 430 °C for eq 16 and 20, and the resulting spectra of $VO_2(SO_4)_2^{3-}$ and the $VO_2SO_4^-$–$VO(SO_4)_3^{3-}$ system are given in Figure 8. It was not possible to distinguish between the $VO_2SO_4^-$ and the $VO(SO_4)_3^{3-}$ (or $VO_2SO_4S_2O_7^{3-}$) species, as the temperature variation could not be taken into account in the calculation. The results of the calculations are given in Table V, where also is included the equilibrium constant at 450 °C, based on the potentiometric measurements to be discussed below.

Potentiometric Measurements of V_2O_5 in $K_2S_2O_7$–K_2SO_4 Melts at 410–450 °C. In Table VI are given the values for mole fractions, concentrations, and cell potentials for 0.15, 0.5, and 0.7 mol/L V(V) (added as V_2O_5) in $K_2S_2O_7$–K_2SO_4 at 410–450 °C. The compositions are corrected for the small amount of K_2SO_4 initially present in the pyrosulfate. Plots of the average experimental coordination number, $\bar{n}$, as a function of the pSO_4^{2-} values calculated at 450 °C and 0.15 mol/L V(V) from Table VI are shown in Figure 9A. From this figure it is seen that the value of $\bar{n}$ increases with increasing sulfate content of the melt, and it seems that equilibria are involved between vanadium(V) species with $\bar{n}$ values between

0 and 1. It is also interesting to note that $\bar{n}$ apparently is independent of both the concentration of vanadium(V) and the temperature in the investigated ranges (Figure 9A-F). This supports strongly the spectrophotometric evidence that only monomeric vanadium(V) species are present in the melts under investigation. Furthermore, the spectrophotometric conclusion that the ratio $VO_2SO_4^-$:$VO(SO_4)_3^{3-}$ is temperature dependent is indirectly confirmed, as $\bar{n}$ for both $VO_2SO_4^-$ and $VO(SO_4)_3^{3-}$ (or $VO_2SO_4S_2O_7^{3-}$) is zero. Hence, no shift in $\bar{n}$ would be observed as a function of temperature.

It is, however, clear that a fairly large number of vanadium species with $\bar{n}$ in the range 0-1 can be imagined. Of these, vanadates can be ruled out since they are only found in strongly basic media. Polymeric species can generally be ruled out on the basis of the invariance of $\bar{n}$ with concentration and from the spectral behavior. Further, the found $\bar{n}$ values are in the range 0-1 and the found ν values in the range 0-2. Since $\bar{n}$ and ν are interrelated, only the following single-species dissolution reactions (giving rise to formation of oxo sulfato complexes) are possible within these ranges:

$$V_2O_5 + nS_2O_7^{2-} \rightarrow 2VO_{(5-n)/2}(SO_4)_n^{n-} \quad (21)$$

$$\bar{n} = 0 \text{ and } \nu = 2$$

$$V_2O_5 + nS_2O_7^{2-} + 2SO_4^{2-} \rightarrow 2VO_{(5-n)/2}(SO_4)_{n+1}^{(n+2)-} \quad (22)$$

$$\bar{n} = 1 \text{ and } \nu = 0$$

In these reactions n is furthermore restricted to be an uneven integer with the values 1 and 3 only, since a value of 5 implies the coordination of the small V^{5+} ion to 5 or 6 sulfate ions. This gives altogether the species $VO_2SO_4^-$, $VO(SO_4)_3^{3-}$, $VO_2(SO_4)_2^{3-}$, and $VO(SO_4)_4^{5-}$. Because of the large negative charge, $VO(SO_4)_4^{5-}$ is not probable. It can now be seen that the species left are the same as given in eq 16 and 20.

This result does in fact not contradict the already mentioned investigation[16] of V_2O_5 in molten NH_4HSO_4 at 200 °C. It was concluded here that the species VO_2^+ is formed in an acidic medium and $VO_2SO_4^-$ in basic. It is not clear, however, that these really are the species formed, but the investigation confirms that an exchange of sulfate ions is taking place, and this exchange is acid/base controlled. It is further interesting to note that recently Glazyrin et al.[41] from an examination of the phase diagram for V_2O_5-$K_2S_2O_7$ and on the basis of IR spectroscopy proposed the existence of the compounds KVO_2SO_4, $K_4(VO_2)_2(SO_4)_2S_2O_7$, and $K_3VO_2SO_4S_2O_7$. It can be seen that the anions for two of these compounds are identical with the ones proposed in the present paper (i.e., with $VO(SO_4)_3^{3-}$ given in the isomeric form $VO_2SO_4S_2O_7^{3-}$).

The curved lines in Figure 9 are drawn with the assumption that eq 20 represents the system. Due to the small change in $[S_2O_7^{2-}]$, this model could not be distinguished from eq 16. The result of the calculations is already shown in Table V, and a close agreement with the spectrophotometric results is observed.

Acknowledgment. The authors wish to thank Dr. M. Gaune-Escard, Université de Provence, for providing us with the calorimetric data for $K_2S_2O_7$. Further thanks are due to Statens tekniskvidenskabelige Forskningsråd for financial support.

Registry No. K_2SO_4, 7778-80-5; $K_2S_2O_7$, 7790-62-7; V_2O_5, 1314-62-1.

(41) Glazyrin, M. P.; Krasil'nikov, V. N.; Ivakin, A. A. *Zh. Neorg. Khim.* **1980**, *25*, 3368.

Contribution from the Department of Chemistry, University of New Orleans, New Orleans, Louisiana 70122

Photolysis of Matrix-Isolated Hydridotetracarbonylcobalt(I). Comparison of the Probabilities of Carbonyl Loss with Hydrogen Atom Loss

RAY L. SWEANY

Received June 29, 1981

The photolysis of $HCo(CO)_4$ in CO matrices can be accounted for by two processes. A process of CO loss is observed as CO exchange in ^{13}CO matrices, and a process of metal-hydrogen bond homolysis is observed especially when the CO loss process is suppressed. The relative quantum yields have been estimated to be eight losses of CO for every loss of hydrogen with use of 254-nm radiation. The first electronic transition that is observed for $HCo(CO)_4$ is at 227 nm, which is assigned to be the LMCT from the hydrogen. This assignment is consistent with the intensity of the transition, the observed photochemistry, and several calculations of the ground-state electronic structure that have appeared in the literature.

The photolysis of $HCo(CO)_4$ in matrices shows evidence of metal-hydrogen bond homolysis.[1] Also, it is apparent that $HCo(CO)_3$ is formed in argon matrices, although the infrared band assigned to $HCo(CO)_3$ is less intense than those observed for $Co(CO)_4$. Taken at face value, it would seem that the quantum yield for hydrogen atom loss is larger than that for CO loss. However, such an analysis ignores the possibility of fragment recombination during photolysis. Previously, I attempted to elucidate the cage effect for the hydrogen atom loss process as described by eq 1. It was concluded that the

$$HCo(CO)_4 \rightarrow H\cdot + \cdot Co(CO)_4 \quad (1)$$

photolysis event that is not reversed is that which results from the hydrogen atom being ejected from the immediate vicinity of $Co(CO)_4$. It was not then possible to discuss the cage effect for CO loss, as described by eq 2. This paper reports the

$$HCo(CO)_4 \rightarrow HCo(CO)_3 + CO \quad (2)$$

results of isotope exchange studies, which indicate a large cage effect for reaction 2. The major result of photolysis of $HCo(CO)_4$ may well be CO loss, which is efficiently reversed in both argon and CO matrices. In this respect $HCo(CO)_4$ resembles $HMn(CO)_5$[2,3] and $R_3Si(CO)_4$.[4]

Experimental Section

Equipment and procedures for studying matrices of $HCo(CO)_4$ have been described previously.[1] Positions of infrared bands are

(1) Sweany, R. L. *Inorg. Chem.* **1980**, *19*, 3512-3516.

(2) Rest, A. J.; Turner, J. J. *J. Chem. Soc., Chem. Commun.* **1969**, 375-376.

(3) Church, S. P.; Poliakoff, M.; Timney, J. A.; Turner, J. J. *J. Am. Chem. Soc.* **1981**, *103*, 7515.

(4) Reichel, C. L.; Wrighton, M. S. *J. Am. Chem. Soc.* **1981**, *103*, 7180.

0020-1669/82/1321-0752$01.25/0